New Results

Selective inhibition of CA IX over CA XII using benzene sulfonamides: Disconnect between CA activity and growth inhibition in breast cancer cells

Mam Y. Mboge[1], Zhijuan Chen[1], Alyssa Wolff[1], John V. Mathias[1], Chingkuang Tu[1], Murat Bozdag[2], Fabrizio Carta[2], Claudiu T. Supuran[2], Robert McKenna[1], and Susan C. Frost[1*]

From the [1]Department of Biochemistry and Molecular Biology, College of Medicine, University of Florida, 1200 Newell Drive, Gainesville, FL 32610, USA; [2]University of Florence, NEUROFARBA Department, Sezione di Farmaceutica e Nutraceutica, Via Ugo Schiff 6, 50019 Sesto Fiorentino (Florence), Italy.

Running title: Selective Inhibition of CA IX over CA XII

Keywords: Benzene sulfonamides, SLC-0111, carbonic anhydrase, tumor microenvironment, breast cancer

Corresponding Author:
Susan C. Frost, Ph.D.
sfrost@ufl.edu
Phone: 3522948386
Department of Biochemistry and Molecular Biology
1200 Newell Drive
University of Florida
Gainesville, FL 32610

Abstract

Carbonic anhydrases (CAs) have been implicated in tumor progression particularly membrane bound CA isoform IX (CA IX). In contrast to CA IX, expression of CA XII, specifically in breast cancer, is associated with a better outcome despite performing the same catalytic function. In this study, we have structurally modeled the orientation of bound ureido-substituted benzene sulfonamides (USBs) within the active site of CA XII, in comparison to CA IX and cytosolic off-target CA II, to understand isoform specific inhibition. This has identified specific residues within the CA active site, which differ between isoforms that are important for inhibitor binding and isoform specificity. The affinity of these inhibitors are two to three orders of magnitude lower in breast cancer cells, that selectively express CA IX or CA XII, relative to recombinant CA proteins. However, we show significantly greater inhibition of CA IX activity over CA XII. While the inhibitors block cell growth, without inducing cell death, this occurs at two orders of magnitude above the K_i values for inhibition of CA IX and CA XII in their respective cell types. Surprisingly, the USBs inhibited cell growth even in cells in which CA IX and CA XII expression was ablated. Despite the potential for these sulfonamides as chemotherapeutic agents, these data suggest that we reconsider the role of CA activity on growth inhibition.

Introduction

Breast cancer remains the second most diagnosed and one of the leading causes of cancer-related deaths among women in the United States. The higher mortality rate observed in women with triple negative breast cancer (TNBC) is attributed to lack of targeted therapies coupled with the inability to treat metastatic disease (1,2). Despite the major advances in therapeutic approaches, metastatic and aggressive breast cancer subtypes, such as TNBC, are difficult to treat. In part, this is because tumors develop resistance to radiation and/or chemotherapies, limiting their effectiveness. Changes in the tumor microenvironment (TM), induced in part by hypoxia, underlie aggressive and resistant cancer phenotypes (3). It is known that the hypoxic TM contributes to tumorigenic characteristics such as tumor cell proliferation, angiogenesis, cell motility, and invasiveness that translate to an overall poor prognosis in cancer patients (3,4). Hypoxia induces a global change in gene expression through stabilization of hypoxia inducible factor one alpha (HIF1α) (5). Stabilization of this transcription factor leads to the upregulation of genes important for cell survival (5). Hypoxia-induced upregulation of genes in glycolysis cause elevated glucose uptake, which is a hallmark for actively dividing cells and correlates closely with transformation (6-8). Increased glycolysis results in high rates of extracellular acidification (pH_e) through the export of H^+ in an attempt to maintain a more basic/neutral intracellular pH (pH_i) (9-11). This increase in H^+ production and export to the extracellular space induces apoptosis in normal cells surrounding tumors, but not the tumor cells themselves, as these conditions actually promote their survival (3,11-13). The stress of the TM also induces resistance to therapeutic drugs, preventing uptake as pH gradients change across the membrane (7). This, in turn, induces the counter transport of drugs reducing concentrations inside cells and thus effectiveness. This is true not only for TNBC patients treated with cytotoxic drugs but also ER- and HER2-positive patients treated with targeted therapies (14).

Important modulators of the hypoxic TM include membrane-bound carbonic anhydrases (CAs), which are zinc metalloenzymes that catalyze the reversible hydration of CO_2 and control extracellular pH to promote tumor cell survival (15-21). In breast cancer, carbonic anhydrase IX (CA IX) expression is upregulated in hypoxic TNBC tissue and is considered a prognostic marker for this phenotype (22-25). The highly aggressive TNBC phenotype accounts for only about ~12% of breast cancers (1) but is responsible for a disproportionate number of breast cancer deaths (2). As mentioned, there is no selective treatment for this refractive disease. By comparison, patients with ER-positive breast cancers have a more favorable prognosis and adjuvant therapy with tamoxifen (a selective estrogen modulator) has contributed to a significant decrease in mortality in that patient population (14). Yet, many of the tamoxifen-treated women develop endocrine resistance and eventually progress to metastatic disease (26,27). In normal cells, CA IX expression is limited primarily to gut epithelium, but is upregulated in many hypoxic tumors including breast cancer (23,26,28-39). CA IX is not only a marker for hypoxia but may also serve as a therapeutic target for the treatment of TNBC patients. CA XII expression, on the other hand, is hypoxia independent and an indicator of better patient outcome, specifically in breast cancer (40). Its expression is under the control of the estrogen receptor and associated with ER-positive breast carcinomas (40-43). CA XII is also expressed more abundantly across tissue types, including normal breast tissue (37,44). This presents a problem, as most CA inhibitors are non-specific, i.e. they target most catalytically active CAs (45). It would therefore be beneficial if CA IX could be selectively targeted over CA XII.

Sulfonamides are the most studied class of CA inhibitors (CAIs) with several compounds in clinical use for the treatment of diseases including glaucoma, altitude sickness, and epileptic seizures (20,46-50). Although these sulfonamides are potent CAIs, most lack isoform selectivity and do not specifically target the tumor-associated isoforms CA IX and CA XII (48). This lack of specificity is attributable to the highly conserved residues within the active site of CAs (45). These similarities have challenged the development of isoform-specific inhibitors, causing competition between isoforms, which reduce efficacy. This is especially true in the case of CA II. This isoform has the widest tissue distribution and is abundantly expressed in red blood cells (representing 5% of all protein) (51,52). As most drugs are delivered systemically and are membrane permeable, it is likely that CA II will sequester CA inhibitors reducing circulating concentrations limiting exposure within tumors. That said, none of the clinical CAIs have been used for the treatment of cancer. Ureido-substituted benzene sulfonamides (USBs) are potent and selective inhibitors of recombinant CA IX and CA XII activity (53-55). X-ray crystallographic studies recently provided insight into the mechanism of USB-mediated selective inhibition of CA IX over CA II (53). Those studies showed that the USBs interact more favorably with residues in the active site of CA IX versus CA II (53). These inhibitors also showed both anti-proliferative and anti-metastatic properties in preclinical models (24,55). One of the USBs (SLC-0111) recently completed phase I clinical trials and is scheduled to begin phase II trials for the treatment of solid tumors that over express CA IX (clinical trials.gov, NCT02215850).

The goal of this study was to distinguish the mechanistic effects of USB-mediated inhibition of CA IX and CA XII in the context of breast cancer cells. To accomplish this, three USBs (including SLC-0111) were studied using *in-silico* modeling to understanding binding mechanisms and their efficacy was tested in cell lines representing TNBC and ER-positive breast cancers. Using this approach, differences in residues within the active sites of CA IX and CA XII indicated that these drive isoform-specific interactions affecting affinity of the USBs. The USB compounds were also shown to inhibit CA activity with surprising specificity for CA IX in TNBC cells, relative to CA XII in ER-positive cells given similar K_i values for purified protein. This same specificity appears to drive USB-mediated growth inhibition. Yet the K_i values for inhibiting catalytic activity in CA IX and CA XII in cells is 2 and 3 orders, respectively, less efficacious than would be expected based on activity studies using purified protein and binding kinetics based on structures. In addition, growth inhibition requires even higher concentrations of inhibitors than that needed for inhibition of activity in cells. Further, cells that lack expression of CA IX or CA XII are still sensitive to USB-mediated inhibition of cell growth. Despite the excellent inhibition of the USBs against purified CA IX and CA XII, and the specificity for CA IX over CA XII in cells, we must consider the possibility that CA activity may not be the target for sulfonamide action with respect to cell growth inhibition.

Results

Isoform selective binding and interaction of USB compounds to CA IX and CA XII.

The structural formulae of the USB inhibitors used in this study and their respective K_i values for recombinant CA II, IX and XII are provided in Table 1 (53-55). These data show the USB compounds selectively bind to and inhibit the tumor-associated isoforms CA IX and XII relative to the off-target CA II (53-55). Cytosolic CA II exists as a monomer (Figure 1A), while both membrane-bound CA IX and CA XII have been shown to form dimers (catalytic domains of the dimers are shown in Figure 1C and 1E). Isoform selectivity towards CA IX and CA XII was evident in the differences in K_i values for these isoforms relative to CA II, obtained using Applied Photophysics stopped-flow kinetics of purified recombinant proteins, the CA-catalyzed CO_2 hydration activity recorded with phenol red as a pH indicator (Table 1) (55).

Previously, the crystallographic structures of all three compounds bound to CA II (Figure 1B) and the CA IX-mimic (Figure 1D), have been determined (53). As expected, each compound was shown to directly interact with the zinc ion, via the sulfonamide moiety (53). Because of their extended tail moieties, the USB compounds also interacted with residues, between 10-15 Å away from the zinc, favoring the hydrophobic side of the active (Figure 1B, 1D and 1F). This region is located close to the entrance of the active site and has previously been termed the "selective pocket" (56,57), because it has a clustering of several amino acids differences among CA isoforms (Table 2). Residue 131 (CA II numbering), located within the selective pocket, is different among the isoforms. In CA II, this residue is a phenylalanine (CA II residue numbering will be used throughout the text). Its bulky side chain causes steric hindrance and therefore induces conformation changes of the bound compounds tail groups (Figure 1B, Table 1). In CA IX, residue 131 is a valine, which allows for more favorable binding and therefore greater isoform selectivity towards CA IX compared to CA II (Figure 1D, Table 1). We believe that the differences in the active site residues, located within the selective pocket, are responsible for the observed differences in the K_i values for the bound compounds (Table 1). By comparison, the classical CA inhibitor, acetazolamide, can only interact with the active site zinc ion and with residues within 10 Å of the zinc because of its shorter tail moiety (58). Residues in this region of the active site are among the most conserved between isoforms (45).

We performed *in silico* modeling of the three USB compounds (U-CH_3, U-F and U-NO_2) into the active site of CA XII (Figure 1F). Residue 131 in CA XII is an alanine (Table 2), which like valine (in CA IX) has a small hydrophobic side chain that results in favorable binding and selectivity towards this isoform (Table 1). In addition, CA XII has a serine (polar uncharged side chain) at position 132, which is also located close to the entrance of the active site. As such, this residue also causes steric hindrance, which induces conformational changes in all three sulfonamides, enhancing binding and inhibition (Table 1). In addition, serine 132 and also serine 135 (both charged residues and also unique to CA XII) create a narrow hydrophobic region within the CA XII active site (Figure 1D). This induces an energetically favorable change, especially, in the conformation of compound U-F (relative to CA II and CA IX) within the active site of CA XII. These residues also prevent steric clashes with residue 131 and facilitate compound interactions in the narrow hydrophobic region within the selective pocket. These interactions

and the resulting conformational change in U-F will be specific to CA XII, because neither CA II nor CA IX has serine residues at positions 132 or 135 (Table 2).

Effect of USB inhibitors on CA IX and CA XII activity in breast cancer cells.

To determine the effect of USB compounds on CA activity in breast cancer cells, cell lines that only express CA IX or CA XII at the cell surface were selected. Based on previous work, two lines that showed strong expression of these CAs were used: a newly identified TNBC line (UFH-001) and the T47D line. The T47D line is a well-studied ER-positive, luminal line. UFH-001 cells represent a new TNBC line arising from MCF 10A cells (considered by many as the control line for breast cancer cells) but with a particularly aggressive behavior. Characterization of UFH-001 cell line is described elsewhere (59). When compared to parental MCF 10A cells, UFH-001 cells show greater expression of CA IX protein (Figure 2A) and mRNA (Supplemental Figure S1A) under normoxic conditions. However, under hypoxic conditions both MCF 10A and UFH-001 cells upregulate CA IX expression (Figure 2A). It can also be noted that there is a difference in the migration patterns of CA IX between the two cell lines. In UFH-001 cells CA IX migrates as a doublet with molecular weights of 54 and 58 kDa, both of which are glycosylated (60). However, in MCF 10A CA IX migrates as a singlet with a molecular weight slightly lower than 58 kDa. The observed differences in molecular weight may result from differences or deletions in primary sequence. CA XII expression is limited to the T47D cells (Supplemental Figure S1B and Figure 2B), and is independent of hypoxia (Figure 2B). Expression of cytosolic CA II protein is only observed in UFH-001 cells and is not sensitive to hypoxia (Figure 2A). The upregulation of CA IX in hypoxic UFH-001 cells underlies the increase in cell surface CA activity in hypoxic versus normoxic cells (Figure 2C) (22). That there is no change in CA activity in T47D cells in response to hypoxia relative to normoxia correlates with the lack of induction in CA XII expression (Figure 2D).

The inhibitory capacity of USB compounds U-CH_3, U-F and U-NO_2 (see Table 1) on CA IX and CA XII activity in the two breast cancer cell lines were studied under normoxic and hypoxic conditions. Because UFH-001 cells express both CA II and CA IX, the progress curves that follow CA activity are biphasic (Figure 3A-3C). The first phase (phase I, 20-40 sec after addition of cells) reflects CA II activity. The second phase (phase II, 100-400 sec) reflects CA IX activity. Phase I, in the absence of inhibitors, represents the rapid diffusion of $^{13}C^{18}O_2$ into cells where catalytic cycles deplete ^{18}O from $H^{13}C^{18}O_3$ followed by efflux of $^{13}CO_2$ species from the cell. There is little change in the slope of this phase between normoxic and hypoxic cells, although the length of time in this phase is shortened (Figure 3A-3C). Phase II, in the absence of USB compounds is dominated by hydration-dehydration activity of CO_2/HCO_3^- outside of the cell representing CA IX activity. The first order rate constant of phase II is greater for hypoxic cells compared with normoxic cells (Figure 2C). This indicates a higher rate of CO_2 hydration/dehydration on the extracellular face of hypoxic cells, which we associate with enhanced expression of exofacial CA IX (Figures 2A and 2C).

The results in Figure 3 also show that USB compounds have limited effects on phase I in the UFH-001 progress curves under either normoxic (Figures 3A-C) or hypoxic conditions (results not shown). This means that during the time course of these experiments, the inhibitors did not permeate the membrane to inhibit CA II except at high concentrations of U-F (SLC-0111) which was detected as an increase in the atomic fraction of ^{18}O in $^{13}CO_2$ (starting at ~200 seconds, Figure 3B and supplemental Figure 2B) rather than a loss. All three CA inhibitors had significant effects on phase II of the progress

curve indicative of a decrease in CA IX activity (Figures 3A-C). In other words, the slopes of the phase II progress curve (used to calculate first order rate constants in Figure 2) decline in the presence of the inhibitors. Based on K_i values in normoxic and hypoxic UFH-001 cells, the most potent inhibitor was U-F (SLC-0111) and the least inhibitory was U-NO_2 (Figure 3G). Hypoxia did not significantly affect the efficacy of any of the USB inhibitors.

T47D cells, which express membrane-bound CA XII but not CA II (Figure 2B), exhibit single-phase progress curves (Figure 3D-F). This activity specifically reflects exofacial CA XII activity. This activity was not sensitive to hypoxia (Figure 2D), which is consistent with lack of CA XII induction (Figure 2B). Like CA IX, USB compounds inhibit CA XII activity (Figure 3D-F). Again, the slope of the progress curve decreases in the presence of the inhibitor. However, there is a striking difference in efficacy that is reflected in a significant increase in the K_i values obtained in T47D cells (Figure 3G) versus UFH-001 cells. Unlike UFH-001 cells, there was little difference in inhibitory effects of the different USB's in T47D cells that again was not affected by normoxic or hypoxic conditions (Figure 3G).

Impact of USB-based inhibitors on breast cancer cell growth, cytotoxicity and apoptosis

MTT, lactate dehydrogenase (LDH), and caspase activity assays were use to test the efficacy of CA IX and CA XII inhibition on breast cancer cell growth and viability. The results show that all three compounds decreased cell growth (MTT assay) in the different cell lines under normoxic conditions (Figure 4, Table 3). No significant trend in compound effectiveness was established between the cells treated for 48 h compared vs 96 h (Figure 4 and Table 3). The most effective compound at inhibiting growth was U-NO_2 in UFH-001 cells (IC_{50} ~25 μM). This compound also inhibited the growth of MCF 10A cells in addition to that of the T47D cells, but requiring nearly three times the concentration compared to UFH-001 cells (Table 3). The MCF 10A cells were the most resistant to compounds U-CH_3 and U-F, with IC_{50} values observed in the range of 500 μM. The concentration to block growth of T47D cells was also in this range at 48 h but improved somewhat at 96 h of exposure (Table 3). We repeated these experiments under hypoxic conditions (Figure 5) with similar results. In addition, we also tested the effects of the USB's on cells in which CA IX or CA XII was knocked out in UFH-001 or T47D cells, respectively. Surprisingly, the result was the same, i.e., the USB's still blocked cell growth at high concentrations.

To specifically test for cytotoxicity, LDH release over 48 h in the presence or absence of the USB compounds were measured. The inhibitors caused only limited cytotoxicity when exposed to cells (Figure 6), relative to a positive control (Supplemental Figure S2). UFH-001 cells were the most sensitive, but only at high concentrations of compound U-NO_2 (Figure 6B). The MCF 10A cells were also somewhat sensitive to U-NO_2 but again at high concentrations (Figure 6A). T47D cells showed no loss of membrane permeability in response to inhibitor treatment (Figure 6C).

These observations led us to question whether the growth arrest and (limited) cytotoxicity observed with the inhibitors was due to the activation of apoptosis. To test this, caspase activity assays were employed. These data revealed that apoptosis was not activated, as caspase activity did not change in either UFH-001 or T47D cells in the presence of USB compounds (Supplemental Figure S3A and S3B, respectively).

Because of the USB-induced growth arrest, their effects on cell cycle transitions were evaluated after exposure to inhibitors for 48 h under normoxic conditions (Figure 7). When compared to T47D cells, the UFH-001 cells were more genomically unstable with ~ 60% of the cells displaying diploidy and the remaining 40% were tetraploid/aneuploid (Figure 7A and 7B). Of the diploid population, ~ 40% of the UFH-001 cells were in G1 phase of the cell cycle and a much lower percentage were in G2 phase. The number of T47D cells in G1 (~ 60%) was significantly higher than the number of cells in the G2 phase of the cell cycle (~ 20%). A significantly higher percentage of cells were observed in G1 phase in T47D compared to UFH-001 cells, while cells in G2 phase were much higher in UFH-001 than T47D cells (Figure 7C). In the presence of USB compounds, there was no change in the number of UFH-001 cells in S phase when compared to the control cells (Figure 7D). However, a significant decrease in the number of T47D cells in S phase was noted with exposure to U-CH_3 and U-F, but not U-NO_2 (Figure 6E). Higher concentrations of U-CH_3 and U-F where used for experiments with T47D cells, because both the K_i values obtained from the MIMS experiments (Figure 7G) and the IC_{50} values obtained from the cell growth assays (Table 3) were much higher for these compounds relative to compound U-NO_2, and by comparison to the more sensitive UFH-001 cells.

Effect of USB inhibitors on CA expression in breast cancer cells

We next examined if inhibition of CA IX and CA XII activity induced an upregulation of the targets or expression of other CA isoforms as a compensatory mechanism. To achieve this, UFH-001 and T47D cells were treated with increasing concentrations of USB compounds for 48 h, under normoxic conditions. Immunoblotting with cell lysates was performed using antibodies against CA II, CA IX and CA XII. No upregulation of other CA isoforms was observed in response to exposure to USB compounds (Supplemental Figure S4). However, there were changes in the endogenously expressed CAs (Supplemental Figure S4). For instance with U-CH_3 treatment, both UFH-001 and T47D cells showed increases in the expression of CA IX and CA XII, respectively, compared to controls (Supplemental Figure S4). Treatment with compound U-F, at lower concentrations (1 μM and 10 μM) increased CA IX and CA XII expression, in UFH-001 and T47D cells, respectively when compared to the control. However, at higher concentrations (100 μM) a decrease in CA IX and CA XII expression was observed (Supplemental Figure S4) and in some cases even to a lesser extent than the control cells (Supplemental Figure S4B). Similar to U-F, compound U-NO_2 also increased somewhat the expression of CA IX and CA XII at lower drug concentrations but ultimately reduced expression, more so with CA IX than CA XII, at concentrations of 100 μM of the compound, when compared to the untreated controls.

Effect of USB inhibitors on cell mobility

While cells grown on polystyrene plates provide useful models, studies of cells grown on more compliant surfaces allow them to recapitulate in part, their behavior *in vivo*. We have taken advantage of Boyden Chambers to monitor cell migration and invasion of UFH-001 and T47D cells in the presence and absence of USB compounds. The results show that only the UFH-001 cells have the ability to migrate and invade which was tested at 24 and 48 h, respectively (Figures 8A and 8C). All three USB compounds blocked UFH-001 cell migration at high concentrations: U-CH_3 and U-NO_2 were the most effective. Significant inhibition of UFH-001 cell invasion was observed with only U-F treatment and at the highest concentration, well above their K_i values for inhibition of activity. Not unexpectedly, we did not observe T47D cell migration and invasion in either the absence or presence of the USBs (Figures 8B and 8D) and

thus we are unable to make a definitive statement regarding any potential effect of the sulfonamide inhibitors on cells that do not possess these features.

Discussion

In the current study, we investigated the binding of a class of USB-based compounds that were specifically designed to inhibit the cancer-associated isoforms, CA IX and CA XII, over the off target CA II. We have shown, as others have previously, that residue 131 is important for isoform selectivity of these compounds towards CA IX and CA XII (53-55,57,61). In addition, our model shows that serine residues 132 and 135 located within the active site of CA XII are required for USB selectivity (compared to the other CAs). This then raises the question: Can we relate these data to the K_i values published for recombinant CAs (55)? Data in Table 1 show that compounds U-CH_3 and U-F exhibit K_i values for CA II that are one to two orders of magnitude greater than for CA IX or CA XII. Our structural data illustrate that these differences are caused by residue 131, which is a phenylalanine in CA II, forcing a lower energy conformation of U-CH_3 and U-F in the active site of CA II (53). This differs from the conformation adopted by inhibitors in CA IX (53) and predicted in CA XII. U-NO_2 conformation is similar among the three CA isoforms, hence the similar K_i values. We must conclude that residue 131 does not cause steric hindrance in the active site of CA II for U-NO_2 but clearly does create steric hindrance for the other two inhibitors. This may be related to physiochemical properties or flexibility of the tail moiety.

In the physiological setting of intact cells, inhibition of CA IX activity by USBs was significantly better than inhibition of CA XII. This was unexpected based on the relatively similar K_i values obtained using recombinant proteins (Table 1) (55). This difference in efficacy was about an order of magnitude between the cell line that expresses CA IX versus the cell line that expresses CA XII. Because of the difference in CA IX and CA XII as prognosticators for patient outcome, this result suggests the potential for selective therapeutic targeting in the clinical setting for CA IX despite the similar efficacy of the drugs with the purified proteins. However, there was also a difference in K_i values between purified protein and those in intact cells. For CA IX, this difference was in the range of two orders of magnitude, depending on the USB. For CA XII, this difference was nearly three orders of magnitude for all USBs. It is possible that part of this difference lies in the use of different techniques for analyzing activity. Recombinant protein activity was measured using stop flow kinetics (55) while enzymatic activity in cells was measured using MIMS, a technique originally developed to define the catalytic mechanisms of purified CAs (60,62), including that for CA IX (63). That differences in the K_i values are based on technique seems unlikely because the rate constants calculated for recombinant CA IX are similar across these techniques (63-65). Further, rate constants determined in isolated membranes containing either CA IX or CA XII (22,66) show strikingly similar values, suggesting that the membrane environment does not influence catalytic activity. Yet, we must also consider that the cellular environment (intact cells) adds layers of complexity relative to even isolated membranes. The cells are in suspension during the MIMS assay, having been released from plates using a non-enzymatic procedure. Thus, many of the cells are still in “colonies” which means that extracellular matrix is still intact. This layer comprised of glycoproteins, proteoglycans, and fibrous proteins like collagen provides a barrier for incoming molecules (like USBs), which potentially reduces their local concentration that could lead to overestimating that concentration.

The effect of the USB inhibitors on cell growth followed a trend similar to that observed for activity, but is more problematic. For both the UFH-001 and T47D cells, the inhibitors were less effective by about two orders of magnitude, based on IC_{50} values. We initially conducted these experiments under

normoxic conditions, even though aggressive forms of cancer exist in hypoxic environments. Our rationale for using normoxia was based on the lack of difference in the K_i values of the USB compounds between normoxic and hypoxic conditions. However, Elena et al. showed that U-F (SLC-0111) activated apoptotic and necrotic programs only in acidified medium (67), a condition associated with hypoxia. But again, these effects were seen at only very high concentration of inhibitor, orders of magnitude above the K_i values for activity. Regardless, we repeated the growth studies with cells exposed to hypoxia but the data were identical. Several studies have shown that the USB compounds are effective at blocking tumor growth (55,68,69), so this is clearly a useful strategy for treating breast cancer patients. Yet, why is there disconnect between the loss of CA activity and the inhibition of cell growth/cytotoxicity? The activity assay is conducted for about 6 min, while the growth, migration/invasion, and cytotoxicity experiments are conducted for up to 96 h. Under these later conditions it is possible that the inhibitors undergo chemical inactivation by oxidation, reduction, or cleavage reducing their ability to block the CAs. It is also possible that the drugs are transported into cells reducing the local concentration around CA IX or CA XII. However, the studies in which we tested USB compounds in cells where CA IX and CA XII were ablated showed the same inhibitory effect of sulfonamides on cell growth. This suggests that, at very high concentrations of the USB's, they are acting independently of their inhibition of CA activity. Indeed others have recently observed this as well (70,71). In these latter studies, investigators identified a potential new sulfonamide target, RMB39 (RNA binding motif protein 39) that is also called CAPERα. They demonstrated that indisulam (an aryl sulfonamide drug in phase II clinical trials for the treatment of advanced stage solid tumors) promotes the recruitment of RBM39 to the CUL4-DCAF15 E3 ubiquitin ligase leading to RBM39 ubiquitination and proteasomal degradation (70,71). Mutations in RBM39 that prevent its recruitment increase its stability, conferring resistance to indisulam's inhibition of cell growth and cytotoxicity (70). Thus, we must consider that CA activity does not regulate cell growth.

In conclusion, we have shown selective binding of USB compounds to recombinant CA IX and CA XII but not to the potential off target CA II. In cells that selectively express either CA IX or CA XII, USB inhibition of activity shows strong specificity for CA IX relative to CA XII. While this correlation holds through to the cell growth studies, the inhibitor IC_{50} values increase by about two orders of magnitude. This disconnect between loss of CA activity and growth inhibition is under further investigation but leads us to question the role of CA activity in cell growth. That said, the inhibitors do block cell growth, so their value as chemotherapeutic agents may still be of considerable value.

Experimental procedures

Ureido-substituted benzene sulfonamide (USB) inhibitors were prepared in dimethyl sulfoxide (DMSO) at stock concentrations of 100 mM and further diluted to appropriate concentrations in cell culture medium before use. Control experiments contain DMSO only. CA II antibody was obtained from Novus Biological (Littleton, CO), CA IX (M75) antibody was a gift from Egbert Oosterwijk, CA XII and GAPDH antibodies were purchased from R&D systems (Minneapolis, MN) and Cell Signaling Technology (Beverly, MA), respectively. All cell lines were authenticated prior to conducting experiments.

In Silico Modeling

X-ray crystallography structures of USB compounds in complex with purified CA II and a CA IX-mimic (analogous site directed mutagenesis of residues in the active site of CA II to resemble CA IX) were previously obtained and published elsewhere (53), but shown for comparison to the modeled CA XII complex in the present study (Figure 1). Each of the USB compounds were superimposed into CA XII structures (PDB ID: 1JCZ) based on the crystal structures of the compounds using Coot (72,73) and adjusted based on steric hindrance constraints.

Cell Culture

MCF 10A cells were cultured in Dulbecco's modified Eagle's medium (DMEM)/Ham's F12 (1:1), supplemented with 5% horse serum, 10 μg/mL insulin, 20 ng/ml epidermal growth factor (EGF) and 100 ng/mL dexamethasone. UFH-001 cells were cultured in DMEM medium supplemented with 10% fetal bovine serum (FBS) and T47D cells were cultured in McCoy's 5A medium supplemented with 10% FBS and 1 mg/mL insulin. All cells were cultured at 37°C in a humidified incubator containing 5% CO_2 and 95% air. For hypoxia treatment, cells were exposed to 1% O_2, 5% CO_2 and balanced N_2 for 16 h using a Billups Rothenberg Metabolic Chamber. Knockdowns of CA IX and CA XII in UFH-001 and T47D cells, respectively, were generated as described and characterized previously (66).

Western Blot Analysis

Western blot analysis was performed, as previously described (23). Cells were collected after drug treatments for 48 h and washed 3x with ice-cold phosphate buffered saline (PBS: 120 mM NaCl, 2.7 mM KCl, 10 mM $NaH_2PO_4.H_2O$ and 10mM Na_2HPO_4 (pH 7.4)) and lysed in RIPA buffer (containing 1% orthovanadate, 25 mM NaF) supplemented with protease inhibitor for 15 min on ice. Lysates were collected and clarified by centrifugation at 55,000 rpm for 60 min at 4°C. Clarified supernatants were collected, and stored at -20°C. Protein concentration was determined using the Markwell modification of the Lowry procedure. Equal amounts of cell lysate (30 μg) were subjected to SDS-polyacrylamide electrophoresis, prepared as described by Laemmli et al. (74) Protein samples were mixed with 2x sample dilution buffer (8% SDS, 4% β-mercaptoethanol, 0.15 mg/mL bromophenol blue, 40% glycerol, 200 mM Tris-base (pH 6.8)). Gels were typically run overnight at room temperature at 40V using a Hoefer S.E. 600 electrophoresis unit. Samples were electrotransferred from SDS-PAGE gels to nitrocellulose membranes in transfer buffer (25 mM Tris-base, 192 mM glycine, 20% methanol) at 200 mA for 2 h at 4°C. After incubation with selective primary and secondary antibodies, proteins were visualized using

ECL reagent according to the manufacturer's directions (GE Healthcare, Wauwatosa, WI). Images were scanned and cropped using Adobe Photoshop version 11.

Enzyme Activity Assay

Catalysis was measured by the exchange of ^{18}O from species of CO_2 into water determined by mass inlet mass spectrometry (MIMS) (62,75). The application of this method in demonstrating exofacial CA activity in TNBC cells has been described previously (60). To decrease inaccuracies arising from ^{12}C-containing CO_2 in cell preparations, ^{13}C- and ^{18}O-enriched CO_2/HCO_3 were used and the rate of depletion of ^{18}O in ^{13}C-containing CO_2 measured. Specifically the atom fraction of ^{18}O in extracellular CO_2 using peak heights from the mass spectrometer was measured: ^{18}O atom fraction [½ (47) + (49)] /[(45) + (47) + (49)], where the numbers in parentheses represent the peak heights of the corresponding masses. Mass spectra were obtained on an Extrel EXM-200 mass spectrometer using electron ionization (70 eV) at an emission current of a 1 mA. Source pressures were 1×10^6 torr. Each of the peaks monitored at masses 45, 47, and 49 were well separated and resolved with a return of ion current (detector response) to the baseline between each mass peak.

Cells were collected from culture plates using cell release buffer (Gibco, Waltham, MA), washed with bicarbonate-free DMEM buffered containing 25 mM Hepes (pH 7.4), and counted. Cells (5.0×10^5 cells/mL, unless otherwise stated) were added to a reaction vessel containing 2 mL of Hepes-buffered, bicarbonate-free DMEM at 16°C in which was dissolved ^{18}O-enriched $^{13}CO^2$ /$H^{13}CO_3$ at 25 mM total $^{13}CO_2$ species. Catalysis by CA in the presence or absence of CA inhibitors was measured after addition of cells (exposed to normoxic or hypoxic conditions) by the exchange of ^{18}O species from species of $^{13}CO_2$ into water determined by measuring CO_2 mass by MIMS as described above. This exchange is a specific measure of CA activity during the time frame of assay. The arrow represents the time at which cells were added to the reaction vessel.

Cell Growth Assay

Cell growth in the presence or absence of compounds was analyzed using 3-[4,5-dimethylthiazol-2-yl]-2,5-diphenyltetrazolium bromide (MTT assays). Briefly, cells were seeded in 96-well plates and treated with different concentrations of compounds after 24 h. The cells were incubated under normoxic conditions under the different treatment conditions for 48 h and 96 h. The medium was replaced every two days. MTT reagent (10% v/v of 5 mg/mL) was added to the cells after each time point and the cells were incubated for an additional 4 h. The medium was removed without disturbing the cells and DMSO was added to each well. The DMSO dissolved cells were incubated while shaking for 15 min in the dark. Absorbance was measured at 570 nm using an Epoch microplate reader (Biotek, Winooski, VT).

Lactate Dehydrogenase Release Assay

Cytotoxicity was estimated using the release of Lactate Dehydrogenase LDH activity (Sigma-Aldrich, St. Louis, MO). Cells were plated in 96-well plates. USB compounds were added the next day. After 48 h, medium was collected from each well to measure the amount of LDH released. The amount of LDH released from each sample was measured at room temperature at 450 nm using a BioTek Epoch microplate reader. LDH activity is reported as nmole/min/mL of medium.

Caspase-3 Activity Assay

Caspase-3 activity assay was performed using an Apo-alert colorimetric caspase assay kit (BioVision, Milpitas, CA). Cells were plated into 10 cm dishes and treated with compounds 24 h later. 48 hrs after various treatments, cells were collected and lysates prepared. Protein concentration was determined and equal volumes of lysates were used for caspase-3 activity assay, measured at 405 nm in a microtiter plate reader using the detection of chromophore p-nitroaniline (pNA) after its cleavage by caspase-3 from the labeled caspase-3 specific substrate, DEVD-pNA. The data are presented as pmol of pNA per µg of cell lysate per hour of incubation. Addition of staurosporine (Sigma-Aldrich, St. Louis, MO) was used as a positive control.

Analysis of Cell Cycle Progression

Cells were seeded in 24-well plates. After 24 h, USB compounds were added to the respective wells and incubated for 48 h. Cells were released with trypsin, harvested and fixed with 500 µL of 50% ethanol in tubes and collected by centrifugation at 13,000 rpm for 5 min. Cell pellets were re-suspended in 500 µL. Propidium iodine (10 µg/mL) containing 300 µg/mL RNase (Invitrogen, Waltham, MA). Then, cells were incubated at room temperature in the dark for 15 min. Cell cycle distribution was obtained using FCS Express Version 5 from De Novo Software (Glendale, CA) using FACS caliber (Becton Dickson, CA).

Cell Migration and Invasion Assays

Serum starved cells were plated at a density of 50,000 cells in 300 µL per insert in 24-well cell migration and invasion plates (Cell BioLabs). The cells were allowed to migrate (24 h) or invade (48 h) from the insert containing serum free medium, with or without USB compounds, towards the well that had medium containing 10% FBS. Fixing and staining cells terminated the assay. Images were then collected and analyzed. All cell lines were maintained at 37°C in humidified air with 5% CO_2 for the duration of the experiment.

Statistical Analysis

Data are presented as means ± SEM. Differences between the treatment groups were analyzed using student's t-test in GraphPad Prism, version 7.0a: p-values < 0.05 was considered statistically significant.

Acknowledgments

The authors would like to recognize the exceptional cell culture skills of Xiao Wei Gu. Financial Support was from the National Institutes of Health, CA165284 (SCF), and minority supplement CA165284-03S1 (MYM) and the UF Cancer Center, Cancer Biology Dissertation Award (MYM). The authors declare that they have no conflicts of interest with the contents of this article.

References

1. Dawood, S., Hu, R., Homes, M. D., Collins, L. C., Schnitt, S. J., Connolly, J., Colditz, G. A., and Tamimi, R. M. (2011) Defining breast cancer prognosis based on molecular phenotypes: results from a large cohort study. *Breast Cancer Res Treat* **126**, 185-192
2. Schneider, B. P., Winer, E. P., Foulkes, W. D., Garber, J., Perou, C. M., Richardson, A., Sledge, G. W., and Carey, L. A. (2008) Triple-negative breast cancer: risk factors to potential targets. *Clin Cancer Res* **14**, 8010-8018
3. Fang, J. S., Gillies, R. D., and Gatenby, R. A. (2008) Adaptation to hypoxia and acidosis in carcinogenesis and tumor progression. *Semin Cancer Biol* **18**, 330-337
4. Verduzco, D., Lloyd, M., Xu, L., Ibrahim-Hashim, A., Balagurunathan, Y., Gatenby, R. A., and Gillies, R. J. (2015) Intermittent hypoxia selects for genotypes and phenotypes that increase survival, invasion, and therapy resistance. *PLoS One* **10**, e0120958
5. Sadri, N., and Zhang, P. J. (2013) Hypoxia-inducible factors: mediators of cancer progression; prognostic and therapeutic targets in soft tissue sarcomas. *Cancers (Basel)* **5**, 320-333
6. Semenza, G. L. (2012) Hypoxia-inducible factors: mediators of cancer progression and targets for cancer therapy. *Trends Pharmacol Sci* **33**, 207-214
7. Brown, J. M. (2007) Tumor hypoxia in cancer therapy. *Methods Enzymol* **435**, 297-321
8. Chiche, J., Brahimi-Horn, M. C., and Pouyssegur, J. (2010) Tumour hypoxia induces a metabolic shift causing acidosis: a common feature in cancer. *J Cell Mol Med* **14**, 771-794
9. Gatenby, R. A., and Gillies, R. J. (2004) Why do cancers have high aerobic glycolysis? *Nat Rev Cancer* **4**, 891-899
10. Neri, D., and Supuran, C. T. (2011) Interfering with pH regulation in tumours as a therapeutic strategy. *Nat Rev Drug Discov* **10**, 767-777
11. Swietach, P., Vaughan-Jones, R. D., and Harris, A. L. (2007) Regulation of tumor pH and the role of carbonic anhydrase 9. *Cancer Metastasis Rev* **26**, 299-310
12. Gatenby, R. A., Gawlinski, E. T., Gmitro, A. F., Kaylor, B., and Gillies, R. J. (2006) Acid-mediated tumor invasion: a multidisciplinary study. *Cancer Res* **66**, 5216-5223
13. Gottlieb, R. A., Giesing, H. A., Zhu, J. Y., Engler, R. L., and Babior, B. M. (1995) Cell acidification in apoptosis - granulocyte-colony-stimulating factor delays programmed cell-death in neutrophils by up-regulating the vacuolar H+-atpase. *P Natl Acad Sci USA* **92**, 5965-5968
14. Abe, O., Abe, R., Enomoto, K., Kikuchi, K., Koyama, H., Masuda, H., Nomura, Y., Sakai, K., Sugimachi, K., Tominaga, T., Uchino, J., Yoshida, M., Haybittle, J. L., Davies, C., Harvey, V. J. *et al.* (2005) Effects of chemotherapy and hormonal therapy for early breast cancer on recurrence and 15-year survival: an overview of the randomised trials. *Lancet* **365**, 1687-1717
15. Chegwidden, W. R., Dodgson, S. J., and Spencer, I. M. (2000) The roles of carbonic anhydrase in metabolism, cell growth and cancer in animals. *Exs* **90**, 343-363
16. Frost, S. C. (2014) Physiological functions of the alpha class of carbonic anhydrases. *Subcell Biochem* **75**, 9-30
17. Gilmour, K. M. (2010) Perspectives on carbonic anhydrase. *Comp Biochem Physiol A Mol Integr Physiol* **157**, 193-197
18. McKenna, R., and Frost, S. C. (2014) Overview of the carbonic anhydrase family. *Subcell Biochem* **75**, 3-5
19. Pastorekova, S., and Pastorek, J. (2004) Cancer-related carbonic anhydrase isozymes and their inhibition. in *Carbonic Anhydrase: Its Inhibitors and Activators* (Supuran, C. T., Scozzafava, A., and Conway, J. eds.), CRC Press, Bocal Raton. pp 255-281
20. Supuran, C. T. (2008) Carbonic anhydrases--an overview. *Curr pharm des* **14**, 603-614
21. Supuran, C. T. (2016) Structure and function of carbonic anhydrases. *Biochem J* **473**, 2023-2032

22. Li, Y., Tu, C., Wang, H., Silverman, D. N., and Frost, S. C. (2011) Catalysis and pH control by membrane-associated carbonic anhydrase IX in MDA-MB-231 breast cancer cells. *J Biol Chem* **286**, 15789-15796
23. Li, Y., Wang, H., Oosterwijk, E., Tu, C., Shiverick, K. T., Silverman, D. N., and Frost, S. C. (2009) Expression and activity of carbonic anhydrase IX is associated with metabolic dysfunction in MDA-MB-231 breast cancer cells. *Cancer Invest* **27**, 613-623
24. Lock, F. E., McDonald, P. C., Lou, Y., Serrano, I., Chafe, S. C., Ostlund, C., Aparicio, S., Winum, J. Y., Supuran, C. T., and Dedhar, S. (2013) Targeting carbonic anhydrase IX depletes breast cancer stem cells within the hypoxic niche. *Oncogene* **32**, 5210-5219
25. Lou, Y., McDonald, P. C., Oloumi, A., Chia, S., Ostlund, C., Ahmadi, A., Kyle, A., Auf dem Keller, U., Leung, S., Huntsman, D., Clarke, B., Sutherland, B. W., Waterhouse, D., Bally, M., Roskelley, C., Overall, C. M., Minchinton, A., Pacchiano, F., Carta, F., Scozzafava, A., Touisni, N., Winum, J. Y., Supuran, C. T., and Dedhar, S. (2011) Targeting tumor hypoxia: suppression of breast tumor growth and metastasis by novel carbonic anhydrase IX inhibitors. *Cancer Res* **71**, 3364-3376
26. Generali, D., Fox, S. B., Berruti, A., Brizzi, M. P., Campo, L., Bonardi, S., Wigfield, S. M., Bruzzi, P., Bersiga, A., Allevi, G., Milani, M., Aguggini, S., Dogliotti, L., Bottini, A., and Harris, A. L. (2006) Role of carbonic anhydrase IX expression in prediction of the efficacy and outcome of primary epirubicin/tamoxifen therapy for breast cancer. *Endocr Relat Cancer* **13**, 921-930
27. Musgrove, E. A., and Sutherland, R. L. (2009) Biological determinants of endocrine resistance in breast cancer. *Nat Rev Cancer* **9**, 631-643
28. Atkins, M., Regan, M., McDermott, D., Mier, J., Stanbridge, E., Youmans, A., Febbo, P., Upton, M., Lechpammer, M., and Signoretti, S. (2005) Carbonic anhydrase IX expression predicts outcome of interleukin 2 therapy for renal cancer. *Clin Cancer Res* **11**, 3714-3721
29. Bui, M. H., Seligson, D., Han, K. R., Pantuck, A. J., Dorey, F. J., Huang, Y. D., Horvath, S., Leibovich, B., Chopra, S., Liao, S. Y., Stanbridge, E., Lerman, M., Palotie, A., Figlin, R., and Belldegrun, A. S. (2003) Carbonic anhydrase IX is an independent predictor of survival in advanced renal clear cell carcinoma: implications for prognosis and therapy. *J Urology* **169**, 172-172
30. Chen, L. Q., Howison, C. M., Spier, C., Stopeck, A. T., Malm, S. W., Pagel, M. D., and Baker, A. F. (2015) Assessment of carbonic anhydrase IX expression and extracellular pH in B-cell lymphoma cell line models. *Leuk Lymphoma* **56**, 1432-1439
31. Chiche, J., Ilc, K., Laferriere, J., Trottier, E., Dayan, F., Mazure, N. M., Brahimi-Horn, M. C., and Pouyssegur, J. (2009) Hypoxia-inducible carbonic anhydrase IX and XII promote tumor cell growth by counteracting acidosis through the regulation of the intracellular pH. *Cancer Res* **69**, 358-368
32. Dorai, T., Sawczuk, I. S., Pastorek, J., Wiernik, P. H., and Dutcher, J. P. (2005) The role of carbonic anhydrase IX overexpression in kidney cancer. *Eur J Cancer* **41**, 2935-2947
33. Genega, E. M., Ghebremichael, M., Najarian, R., Fu, Y., Wang, Y., Argani, P., Grisanzio, C., and Signoretti, S. (2010) Carbonic anhydrase IX expression in renal neoplasms: correlation with tumor type and grade. *Am J Clin Pathol* **134**, 873-879
34. Kivela, A. J., Parkkila, S., Saarnio, J., Karttunen, T. J., Kivela, J., Parkkila, A. K., Pastorekova, S., Pastorek, J., Waheed, A., Sly, W. S., and Rajaniemi, H. (2000) Expression of transmembrane carbonic anhydrase isoenzymes IX and XII in normal human pancreas and pancreatic tumours. *Histochem Cell Biol* **114**, 197-204
35. Kock, L., Mahner, S., Choschzick, M., Eulenburg, C., Milde-Langosch, K., Schwarz, J., Jaenicke, F., Muller, V., and Woelber, L. (2011) Serum carbonic anhydrase IX and its prognostic relevance in vulvar cancer. *Int J Gynecol Cancer* **21**, 141-148
36. Leibovich, B. C., Sheinin, Y., Lohse, C. M., Thompson, R. H., Cheville, J. C., Zavada, J., and Kwon, E. D. (2007) Carbonic anhydrase IX is not an independent predictor of outcome for patients with clear cell renal cell carcinoma. *J Clin Oncol* **25**, 4757-4764

37. Liao, S. Y., Lerman, M. I., and Stanbridge, E. J. (2009) Expression of transmembrane carbonic anhydrases, CAIX and CAXII, in human development. *BMC Dev Biol* **9**, 22
38. Woelber, L., Kress, K., Kersten, J. F., Choschzick, M., Kilic, E., Herwig, U., Lindner, C., Schwarz, J., Jaenicke, F., Mahner, S., Milde-Langosch, K., Mueller, V., and Ihnen, M. (2011) Carbonic anhydrase IX in tumor tissue and sera of patients with primary cervical cancer. *BMC Cancer* **11**, 12
39. Wykoff, C. C., Beasley, N. J., Watson, P. H., Turner, K. J., Pastorek, J., Sibtain, A., Wilson, G. D., Turley, H., Talks, K. L., Maxwell, P. H., Pugh, C. W., Ratcliffe, P. J., and Harris, A. L. (2000) Hypoxia-inducible expression of tumor-associated carbonic anhydrases. *Cancer Res* **60**, 7075-7083
40. Watson, P. H., Chia, S. K., Wykoff, C. C., Han, C., Leek, R. D., Sly, W. S., Gatter, K. C., Ratcliffe, P., and Harris, A. L. (2003) Carbonic anhydrase XII is a marker of good prognosis in invasive breast carcinoma. *Br J Cancer* **88**, 1065-1070
41. Barnett, D. H., Sheng, S., Charn, T. H., Waheed, A., Sly, W. S., Lin, C. Y., Liu, E. T., and Katzenellenbogen, B. S. (2008) Estrogen receptor regulation of carbonic anhydrase XII through a distal enhancer in breast cancer. *Cancer Res* **68**, 3505-3515
42. Creighton, C. J., Cordero, K. E., Larios, J. M., Miller, R. S., Johnson, M. D., Chinnaiyan, A. M., Lippman, M. E., and Rae, J. M. (2006) Genes regulated by estrogen in breast tumor cells in vitro are similarly regulated in vivo in tumor xenografts and human breast tumors. *Genome Biol* **7**, R28
43. Deroo, B. J., and Korach, K. S. (2006) Estrogen receptors and human disease. *J Clin Invest* **116**, 561-570
44. Kummola, L., Hamalainen, J. M., Kivela, J., Kivela, A. J., Saarnio, J., Karttunen, T., and Parkkila, S. (2005) Expression of a novel carbonic anhydrase, CA XIII, in normal and neoplastic colorectal mucosa. *BMC Cancer* **5**, 41
45. Pinard, M. A., Mahon, B., and McKenna, R. (2015) Probing the surface of human carbonic anhydrase for clues towards the design of isoform specific inhibitors. *Biomed Res Int* **2015**, 453543
46. Supuran, C., Dedhar, S., Carta, F., Winum, J. Y., and Mcdonald, P. C. (2012) Carbonic anhydrase inhibitors with antimetastatic activity. Google Patents
47. Supuran, C. T. (2012) Structure-based drug discovery of carbonic anhydrase inhibitors. *J Enzyme Inhib Med Chem* **27**, 759-772
48. Supuran, C. T. (2016) How many carbonic anhydrase inhibition mechanisms exist? *J Enzyme Inhib Med Chem* **31**, 345-360
49. Supuran, C. T. (2017) Advances in structure-based drug discovery of carbonic anhydrase inhibitors. *Expert Opin Drug Discov* **12**, 61-88
50. Supuran, C. T., and Winum, J. Y. (2015) Designing carbonic anhydrase inhibitors for the treatment of breast cancer. *Expert Opin Drug Discov* **10**, 591-597
51. Carter, M. J., and Parsons, D. S. (1970) The purification and properties of carbonic anhydrases from guinea-pig erythrocytes and mucosae of the gastrointestinal tract. *Biochem J* **120**, 797-808
52. Lindskog, S. (1960) Purification and properties of bovine erythrocyte carbonic anhydrase. *Biochim Biophys Acta* **39**, 218-226
53. Mboge, M. Y., Mahon, B. P., Lamas, N., Socorro, L., Carta, F., Supuran, C. T., Frost, S. C., and McKenna, R. (2017) Structure activity study of carbonic anhydrase IX: Selective inhibition with ureido-substituted benzenesulfonamides. *Eur J Med Chem* **132**, 184-191
54. Pacchiano, F., Aggarwal, M., Avvaru, B. S., Robbins, A. H., Scozzafava, A., McKenna, R., and Supuran, C. T. (2010) Selective hydrophobic pocket binding observed within the carbonic anhydrase II active site accommodate different 4-substituted-ureido-benzenesulfonamides and correlate to inhibitor potency. *Chem Commun (Camb)* **46**, 8371-8373

55. Pacchiano, F., Carta, F., McDonald, P. C., Lou, Y., Vullo, D., Scozzafava, A., Dedhar, S., and Supuran, C. T. (2011) Ureido-substituted benzenesulfonamides potently inhibit carbonic anhydrase IX and show antimetastatic activity in a model of breast cancer metastasis. *J Med Chem* **54**, 1896-1902
56. Aggarwal, M., Kondeti, B., and McKenna, R. (2013) Insights towards sulfonamide drug specificity in alpha-carbonic anhydrases. *Bioorg Med Chem* **21**, 1526-1533
57. Pinard, M. A., Boone, C. D., Rife, B. D., Supuran, C. T., and McKenna, R. (2013) Structural study of interaction between brinzolamide and dorzolamide inhibition of human carbonic anhydrases. *Bioorg Med Chem* **21**, 7210-7215
58. Fisher, S. Z., Aggarwal, M., Kovalevsky, A. Y., Silverman, D. N., and McKenna, R. (2012) Neutron diffraction of acetazolamide-bound human carbonic anhydrase II reveals atomic details of drug binding. *J Am Chem Soc* **134**, 14726-14729
59. Chen, Z., Ai, L., Mboge, M. Y., McKenna, R., Frost, C. J., Heldermon, C. D., and Frost, S. C. (2018) UFH-001 cells: A novel triple negative, CAIX-positive, human breast cancer model system. *Cancer Biol Ther*, 1-32
60. Li, Y., Wang, H., Tu, C., Shiverick, K. T., Silverman, D. N., and Frost, S. C. (2011) Role of hypoxia and EGF on expression, activity, localization and phosphorylation of carbonic anhydrase IX in MDA-MB-231 breast cancer cells. *Biochim Biophys Acta* **1813**, 159-167
61. Mahon, B. P., Hendon, A. M., Driscoll, J. M., Rankin, G. M., Poulsen, S. A., Supuran, C. T., and McKenna, R. (2015) Saccharin: a lead compound for structure-based drug design of carbonic anhydrase IX inhibitors. *Bioorg Med Chem* **23**, 849-854
62. Silverman, D. N., and Lindskog, S. (1988) The catalytic mechanism of carbonic anhydrase - implication of a rate limiting protolysis of water. *Acc Chem Res* **21**, 30-36
63. Wingo, T., Tu, C., Laipis, P. J., and Silverman, D. N. (2001) The catalytic properties of human carbonic anhydrase IX. *Biochem Biophys Res Commun* **288**, 666-669
64. Alterio, V., Vitale, R. M., Monti, S. M., Pedone, C., Scozzafava, A., Cecchi, A., De Simone, G., and Supuran, C. T. (2006) Carbonic anhydrase inhibitors: X-ray and molecular modeling study for the interaction of a fluorescent antitumor sulfonamide with isozyme II and IX. *J Am Chem Soc* **128**, 8329-8335
65. Vullo, D., Franchi, M., Gallori, E., Pastorek, J., Scozzafava, A., Pastorekova, S., and Supuran, C. T. (2003) Carbonic anhydrase inhibitors: inhibition of the tumor-associated isozyme IX with aromatic and heterocyclic sulfonamides. *Bioorg Med Chem Lett* **13**, 1005-1009
66. Chen, Z., Ai, L., Mboge, M. Y., Tu, C., McKenna, R., Brown, D. B., Heldermon, C. D., and Frost, C. J. (2018) Differential expression and function of CAIX and CAXII in breast cancer: a comparison between tumorgraft models and cells. *PLoS One.* In Press
67. Andreucci, E., Peppicelli, S., Carta, F., Brisotto, G., Biscontin, E., Ruzzolini, J., Bianchini, F., Biagioni, A., Supuran, C. T., and Calorini, L. (2017) Carbonic anhydrase IX inhibition affects viability of cancer cells adapted to extracellular acidosis. *J Mol Med (Berl)* **95**, 1341-1353
68. Lou, Y., McDonald, P. C., Oloumi, A., Chia, S., Ostlund, C., Ahmadi, A., Kyle, A., auf dem Keller, U., Leung, S., Huntsman, D., Clarke, B., Sutherland, B. W., Waterhouse, D., Bally, M., Roskelley, C., Overall, C. M., Minchinton, A., Pacchiano, F., Carta, F., Scozzafava, A., Touisni, N., Winum, J., Supuran, C. T., and Dedhar, S. (2011) Targeting tumor hypoxia: suppression of breast tumor growth and metastasis by novel carbonic anhydrase IX inhibitors. *Cancer Res* **71**, 3364-3376
69. Touisni, N., Maresca, A., McDonald, P. C., Lou, Y., Scozzafava, A., Dedhar, S., Winum, J. Y., and Supuran, C. T. (2011) Glycosyl coumarin carbonic anhydrase IX and XII inhibitors strongly attenuate the growth of primary breast tumors. *J Med Chem* **54**, 8271-8277
70. Han, T., Goralski, M., Gaskill, N., Capota, E., Kim, J., Ting, T. C., Xie, Y., Williams, N. S., and Nijhawan, D. (2017) Anticancer sulfonamides target splicing by inducing RBM39 degradation via recruitment to DCAF15. *Science* **356**

71. Uehara, T., Minoshima, Y., Sagane, K., Sugi, N. H., Mitsuhashi, K. O., Yamamoto, N., Kamiyama, H., Takahashi, K., Kotake, Y., Uesugi, M., Yokoi, A., Inoue, A., Yoshida, T., Mabuchi, M., Tanaka, A., and Owa, T. (2017) Selective degradation of splicing factor CAPERalpha by anticancer sulfonamides. *Nat Chem Biol* **13**, 675-680
72. Debreczeni, J. E., and Emsley, P. (2012) Handling ligands with Coot. *Acta Crystallogr D Biol Crystallogr* **68**, 425-430
73. Emsley, P., and Cowtan, K. (2004) Coot: model-building tools for molecular graphics. *Acta Crystallogr D Biol Crystallogr* **60**, 2126-2132
74. Laemmli, U. K. (1970) Cleavage of structural proteins during the assembly of the head of bacteriophage T4. *Nature* **227**, 680-685
75. Silverman, D. N. (1982) Carbonic anhydrase: oxygen-18 exchange catalyzed by an enzyme with rate-contributing proton-transfer steps. *Methods Enzymol* **87**, 732-752

Table 1. Inhibition constant (K_i) values for recombinant human CA II, IX, and XII with ureido-substituted benzene sulfonamide compounds **U-CH$_3$, U-F,** and **U-NO$_2$** obtained from Applied Photophysics stopped-flow kinetics experiments.

Compound	***K*$_i$ (nM) ± 5% error**		
	CA II	**CA IX**	**CA XII**
U-CH$_3$ 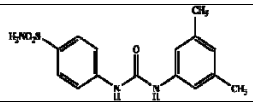	1765	7	6
U-F 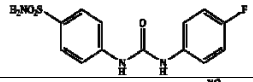	960	45	4
U-NO$_2$ 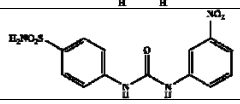	15	1	6

K_i values obtained from Pacchiano et al. (54,55)

Table 2. Resides within the active site of human CA II, CA IX and CA XII that differ between all three isoforms and make up the selective pocket (*CA II numbering*).

Residues in Selective Region	**CA II**	**CA IX**	**CA XII**
67	Asn	Gln	Lys
91	Ile	Leu	Thr
131	Phe	Val	Ala
132	Gly	Ala	Ser
135	Val	Leu	Ser

Information adapted from Pinard et al. (45)

Table 3. IC_{50} values for compounds **U-CH_3, U-F,** and **U-NO_2** in MCF 10A, UFH-001 and T47D cells obtained from MTT assay experiments.

Cell Lines	**MCF 10A Cells**		**UFH-001 Cells**		**T47D Cells**	
Treatment	**48 hrs**	**96 hrs**	**48 hrs**	**96 hrs**	**48 hrs**	**96 hrs**
U-CH_3 (μM)	491 ± 10	508 ± 10	80 ± 2	74 ± 1	330 ± 10	101 ± 10
U-F (μM)	550 ± 10	550 ± 10	62 ± 1	51± 1	537± 10	252 ± 20
U-NO_2 (μM)	64 ± 1	69 ± 1	26 ± 1	20 ± 1	61 ± 1	78 ± 1

Figure Legends

Figure 1. USBs bound in the active site of CAs. Panel A. Ribbon diagram of monomeric CA isoform II (grey). Panel C. Ribbon diagram of the catalytic domains of dimeric CA isoform IX (cyan). Panel E. Ribbon diagram of the catalytic domains of dimeric CA isoform. XII (wheat). Surface representation of compounds U-CH_3 (pink), U-F (green) and U-NO_2 (yellow) in complex with monomers CA II (Panel B), the CA IX-mimic (Panel D), and modeled into the active site of CA XII (Panel F). Catalytic zinc (magenta sphere), hydrophilic (blue) and hydrophobic (orange) residues are as shown. Red double-headed arrows indicate isoform specificity relative to residue 131 (labeled in white). These arrows also show flexibility in tail conformations seen in CA II and CA IX but not in CA XII. The K_i values of each compound bound to purified CA II, CA IX and CA XII are noted next to the inhibitor name. Figures were designed using PyMol.

Figure 2. CA expression and activity in breast cell lines. Panel A. protein expression in a normal immortalized basal type breast cell line (MCF 10A) and a triple negative breast cancer cell line (UFH-001), using western blot analysis (under normoxic (N) or hypoxic conditions (H) for 16 h), respectively. Panel B. Immunoblots for CAs II, IX and XII protein expression in MCF 10A and a luminal breast cancer cell line (T47D). Panel C. UFH-001 and D) T47D cells were grown for 3 days at which point they were exposed to normoxia or 16 h of hypoxia and the cells assayed for CA IX and XII activity, respectively using MIMS. First order rate constants were determined for phase 2 activities and represented. These data represent three independent experiments and as mean ± SEM.

Figure 3. Effects of USBs on CA IX and CA XII activity in breast cancer cell lines. Panels A-C. UFH-001 cells were grown for 4 days under normoxic conditions. CA IX activity (1.0×10^6 cells/mL) was assayed using MIMS in the presence or absence of U-CH_3 (Panel A), U-F (Panel B) and U-NO_2 (Panel C). Panels D-F. T47D cells prepared similarly to UFH-001 cells, but cultured for 6 days, were also assayed for CA XII activity (0.5×10^6 cells/mL) in the absence or presence of the same USB based inhibitors: U-CH_3 (Panel D), U-F (Panel E) and U-NO_2 (Panel F). Atom fractions of ^{18}O in CO_2 were collected continuously. For ease of illustration, data points at 25-s intervals are shown. Phase I in UFH-001 cells indicate CA II activity and Phase II indicate CA IX activity. In T47D cells is representative of CA XII activity. Arrows indicate time point at which cells were added. Panel G. K_i values of each compound in UFH-001 and T47D cells, under normoxic or hypoxic (16 h) conditions, are shown. Data are representative of at least duplicate experiments and as mean ± SEM.

Figure 4. **Effects of USBs on breast cancer cell growth.** Breast cancer cell lines grown under normal culture conditions for 24 h were exposed to compounds for 48 h [U-CH_3 (Panel A), U-F (Panel B), U-NO_2 (Panel D)] or 96 h [U-CH_3 (Panel D), U-F (Panel E), or U-NO_2 (Panel F)]. The MTT assay was performed at 48 and 96 h respectively. Data shown represent at least three independent experiments and are represented as mean ± SEM.

Figure 5. Effects of USBs on cell growth in the presence and absence of hypoxia or in CA knockout cells. One day after plating, breast cancer cell lines were exposed to normoxic (N) or hypoxic (H) conditions for 48 h in the presence of U-CH_3, U-F, or U-NO_2 at the given concentrations in UFH-001 EV cells (Panel A), UFH-001 KO cells (Panel B), T47D EV cells (Panel C) and T47D KO cells (Panel D).

The MTT assay was performed and shown as % cell growth. Data shown represent at least three independent experiments and are shown as mean ± SEM.

Figure 6. **Effects of USBs on breast cancer cell viability.** The cytotoxic effects of USBs were evaluated using an LDH release assay. A) MCF 10A, B) UFH-001 and C) T47D cells were grown in 96-well plates and exposed to U-CH_3, U-F or U-NO_2 for 48 h, under normoxic conditions. LDH release was assayed after treatment, results were evaluated and data analyzed using Prism. Data shown are representative of three independent experiments and as mean ± SEM, *$p < 0.05$.

Figure 7. **Effects of USBs on cell cycle transition in breast cancer cells.** Cell cycle analysis was performed in A) UFH-001 and B) T47D cells treated with varying concentrations of USB compounds for 48 h, under normoxic conditions. Post treatment cells were stained with Propidium Iodine containing RNase A, data was obtained using the FACS caliber instrument and results analyzed with FCS Express and ModFit LT softwares. The percentage of breast cancer cells in C) G-phase, D and E) S-phase in UFH-001 and T47D cells, respectively, were quantified using Prism. Data are represented as mean of at least three independent experiments ± SEM and NC = negative control.

Figure 8. Effects of USBs on breast cancer cell migration and invasion. Serum starved UFH-001 and T47D cells were allowed to either migrate for 24 h or invade for 48 h towards a chemoattractant in the presence or absence of USB compounds. Bright-field images of migrating and invading cells are shown in Panel A (UFH-001 cells) and Panel B T47D cells). Data are quantified for UFH-001 and T47D cells Panel C (migration) and Panel D (invasion). NC= negative control. Data shown are an average of duplicate experiments ± SEM. *$p < 0.05$, and ***$p < 0.001$.

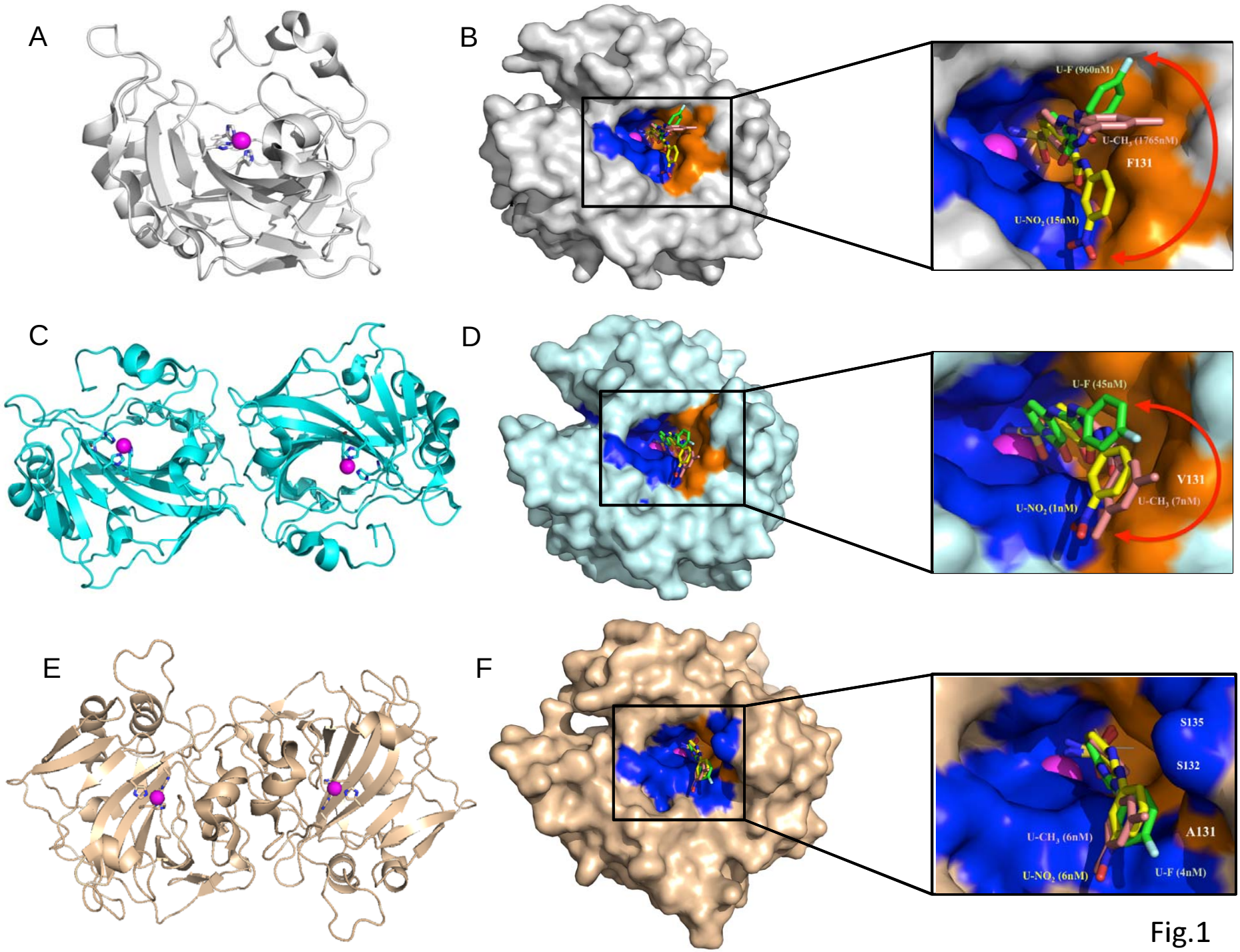
A
B
U-F (960nM)
U-CH3 (1765nM)
F131
U-NO2 (15nM)
C
D
U-F (45nM)
V131
U-CH3 (7nM)
U-NO2 (1nM)
E
F
S135
S132
A131
U-CH3 (6nM)
U-NO2 (6nM)
U-F (4nM)

Fig.1

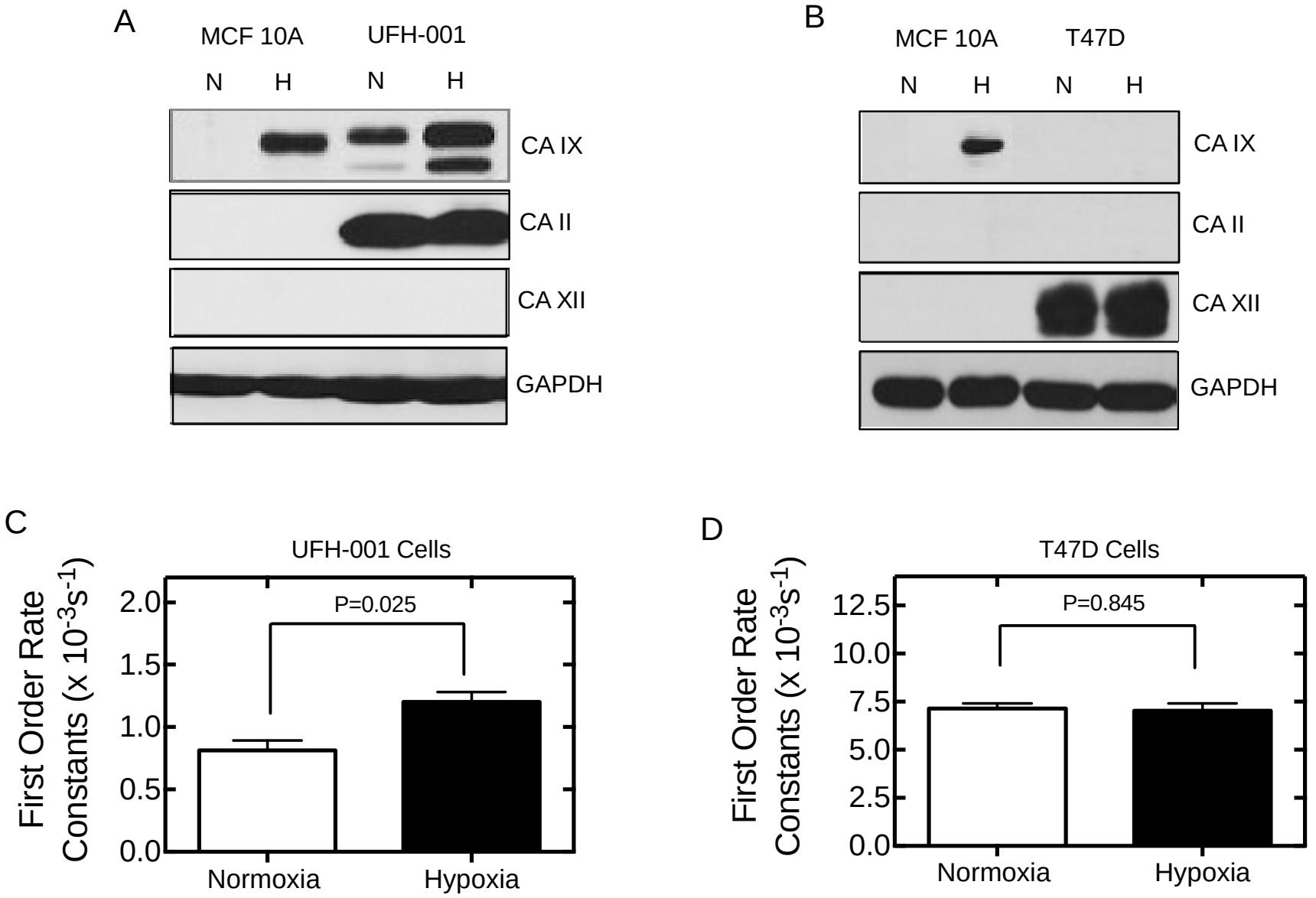
A
MCF 10A
UFH-001
N
H
N
H
CA IX
CA II
CA XII
GAPDH
B
MCF 10A
T47D
N
H
N
H
CA IX
CA II
CA XII
GAPDH
C
UFH-001 Cells
First Order Rate Constants (x 10-3s-1)
P=0.025
2.0
1.5
1.0
0.5
0.0
Normoxia
Hypoxia
D
T47D Cells
First Order Rate Constants (x 10-3s-1)
P=0.845
12.5
10.0
7.5
5.0
2.5
0.0
Normoxia
Hypoxia

Fig.2

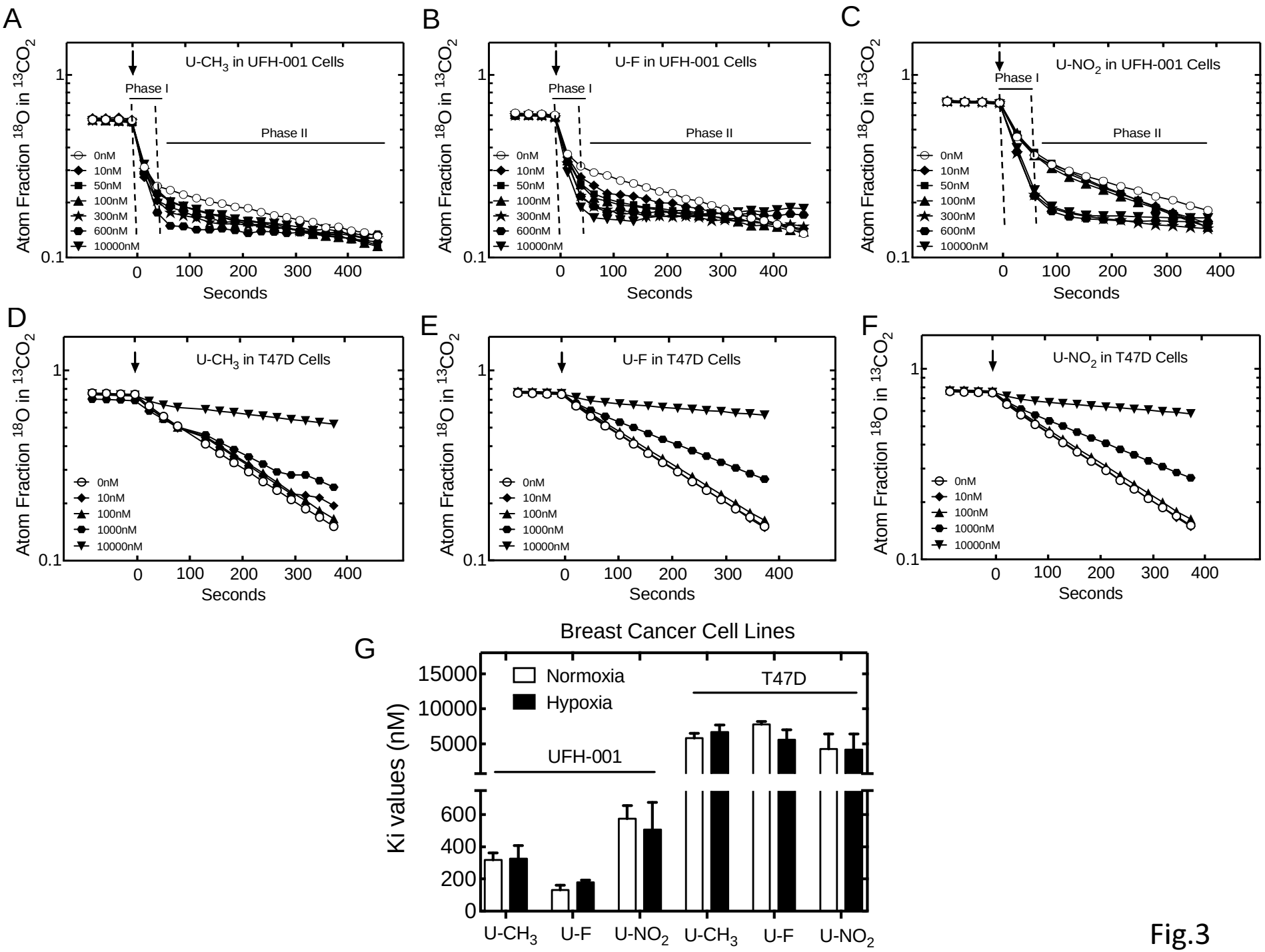
A
U-CH3 in UFH-001 Cells
Phase I
Phase II
0nM
10nM
50nM
100nM
300nM
600nM
10000nM
Atom Fraction 18O in 13CO2
Seconds
B
U-F in UFH-001 Cells
C
U-NO2 in UFH-001 Cells
D
U-CH3 in T47D Cells
1000nM
E
U-F in T47D Cells
F
U-NO2 in T47D Cells
G
Breast Cancer Cell Lines
Normoxia
Hypoxia
T47D
UFH-001
Ki values (nM)
U-CH3
U-F
U-NO2

Fig.3

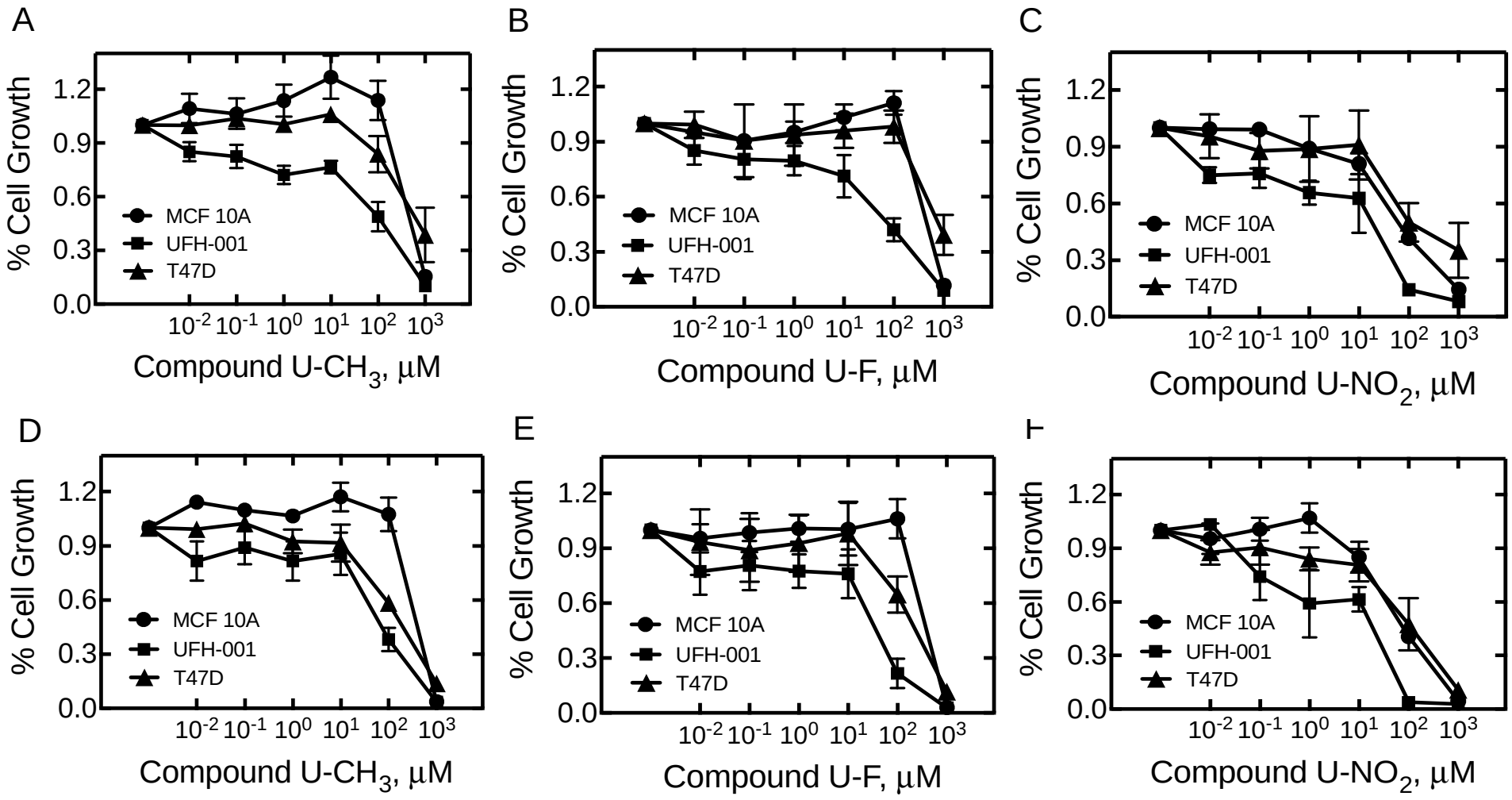
A
B
C
D
E
F
% Cell Growth
1.2
0.9
0.6
0.3
0.0
MCF 10A
UFH-001
T47D
10^{-2} 10^{-1} 10^{0} 10^{1} 10^{2} 10^{3}
Compound U-CH_3, μM
Compound U-F, μM
Compound U-NO_2, μM

Fig.4

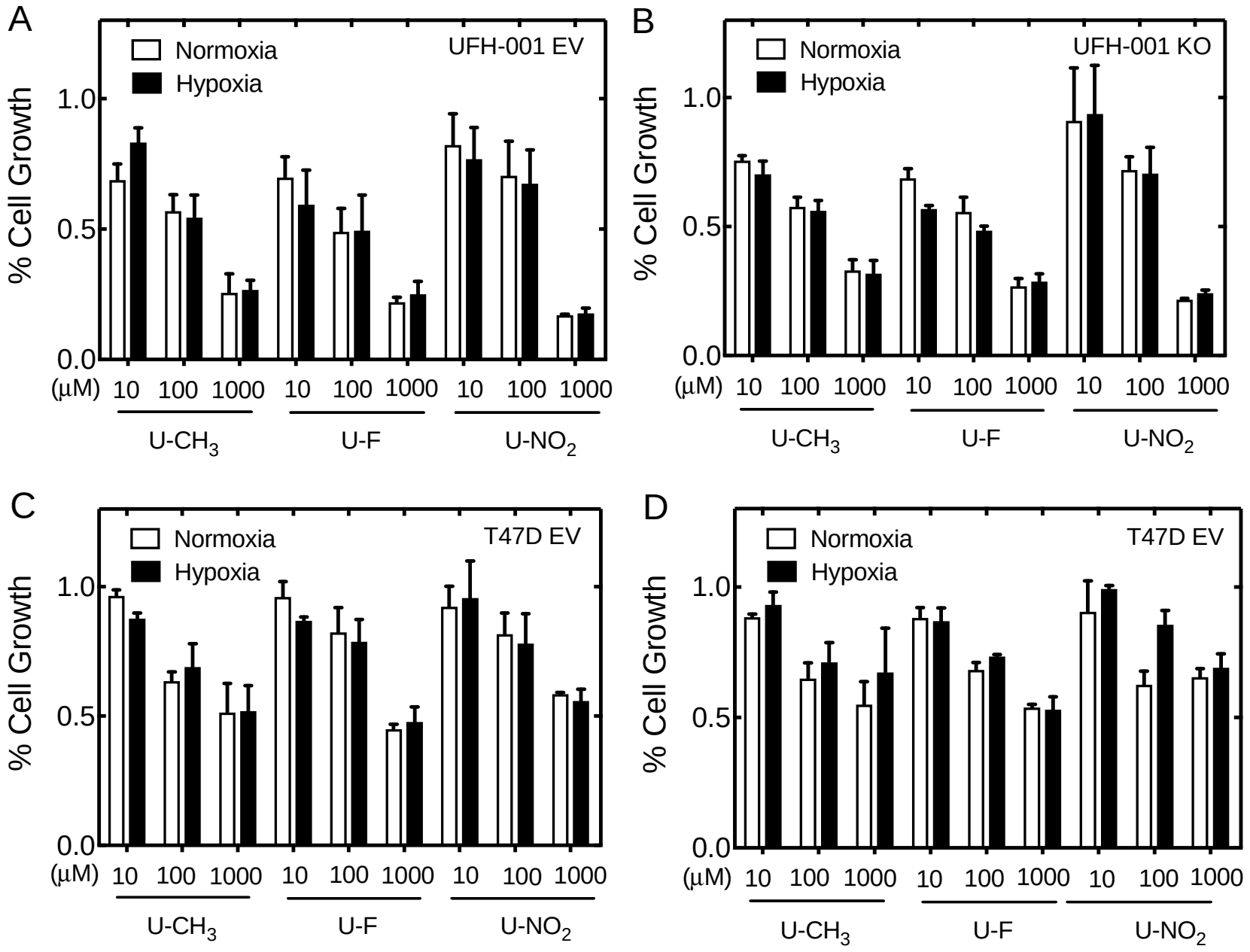
A
Normoxia
Hypoxia
UFH-001 EV
% Cell Growth
1.0
0.5
0.0
(μM) 10 100 1000 10 100 1000 10 100 1000
U-CH3
U-F
U-NO2
B
Normoxia
Hypoxia
UFH-001 KO
% Cell Growth
1.0
0.5
0.0
(μM) 10 100 1000 10 100 1000 10 100 1000
U-CH3
U-F
U-NO2
C
Normoxia
Hypoxia
T47D EV
% Cell Growth
1.0
0.5
0.0
(μM) 10 100 1000 10 100 1000 10 100 1000
U-CH3
U-F
U-NO2
D
Normoxia
Hypoxia
T47D EV
% Cell Growth
1.0
0.5
0.0
(μM) 10 100 1000 10 100 1000 10 100 1000
U-CH3
U-F
U-NO2

Fig.5

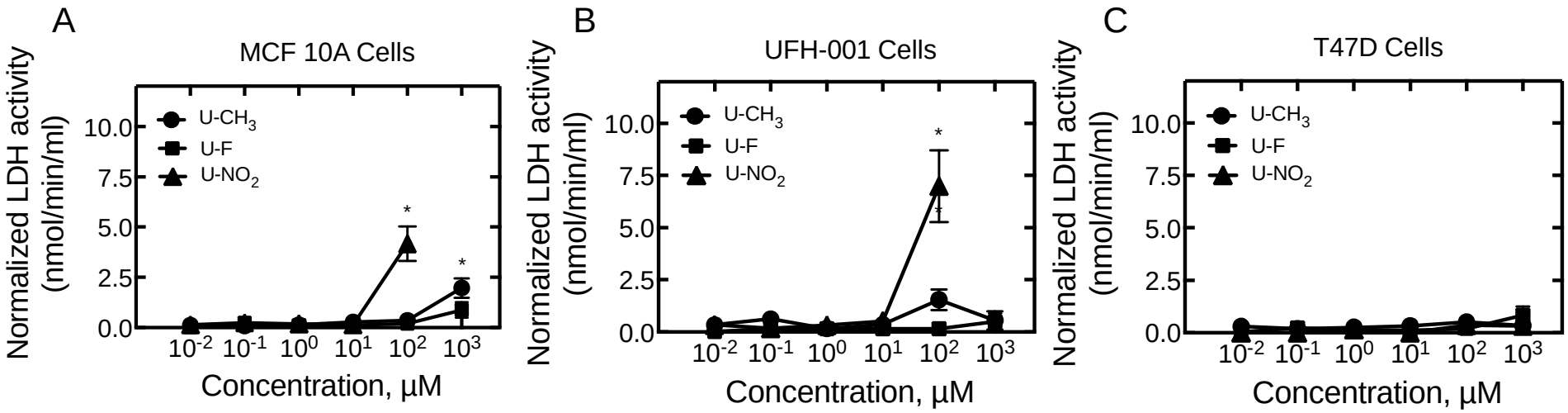
A
MCF 10A Cells
Normalized LDH activity (nmol/min/ml)
U-CH3
U-F
U-NO2
10.0
7.5
5.0
2.5
0.0
*
*
10-2 10-1 100 101 102 103
Concentration, μM
B
UFH-001 Cells
Normalized LDH activity (nmol/min/ml)
U-CH3
U-F
U-NO2
10.0
7.5
5.0
2.5
0.0
*
10-2 10-1 100 101 102 103
Concentration, μM
C
T47D Cells
Normalized LDH activity (nmol/min/ml)
U-CH3
U-F
U-NO2
10.0
7.5
5.0
2.5
0.0
10-2 10-1 100 101 102 103
Concentration, μM

Fig.6

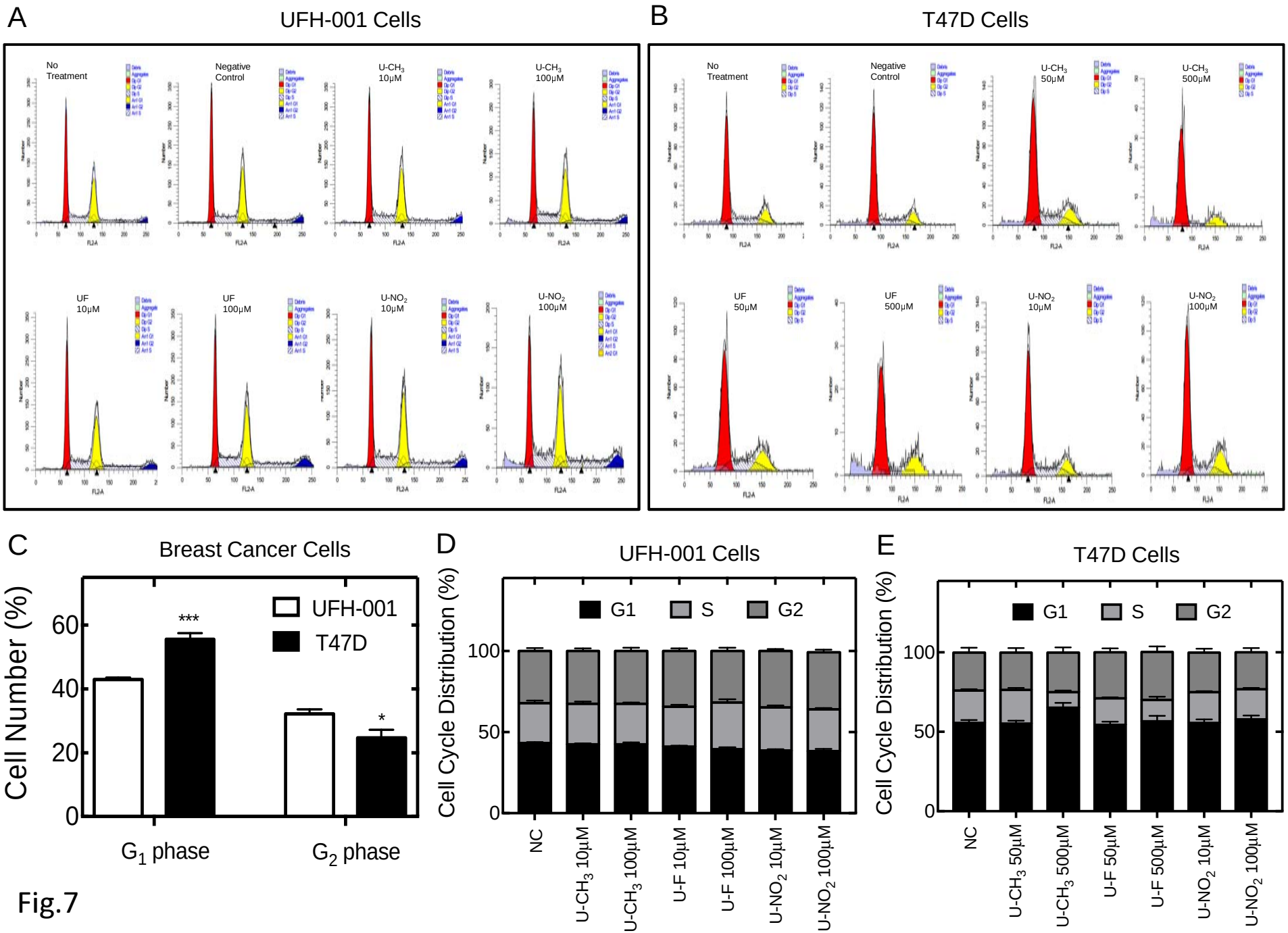
A
UFH-001 Cells
No Treatment
Negative Control
U-CH3 10μM
U-CH3 100μM
UF 10μM
UF 100μM
U-NO2 10μM
U-NO2 100μM
B
T47D Cells
No Treatment
Negative Control
U-CH3 50μM
U-CH3 500μM
UF 50μM
UF 500μM
U-NO2 10μM
U-NO2 100μM
C
Breast Cancer Cells
Cell Number (%)
UFH-001
T47D
***
*
G1 phase
G2 phase
D
UFH-001 Cells
Cell Cycle Distribution (%)
G1
S
G2
NC
U-CH3 10μM
U-CH3 100μM
U-F 10μM
U-F 100μM
U-NO2 10μM
U-NO2 100μM
E
T47D Cells
Cell Cycle Distribution (%)
G1
S
G2
NC
U-CH3 50μM
U-CH3 500μM
U-F 50μM
U-F 500μM
U-NO2 10μM
U-NO2 100μM

Fig.7

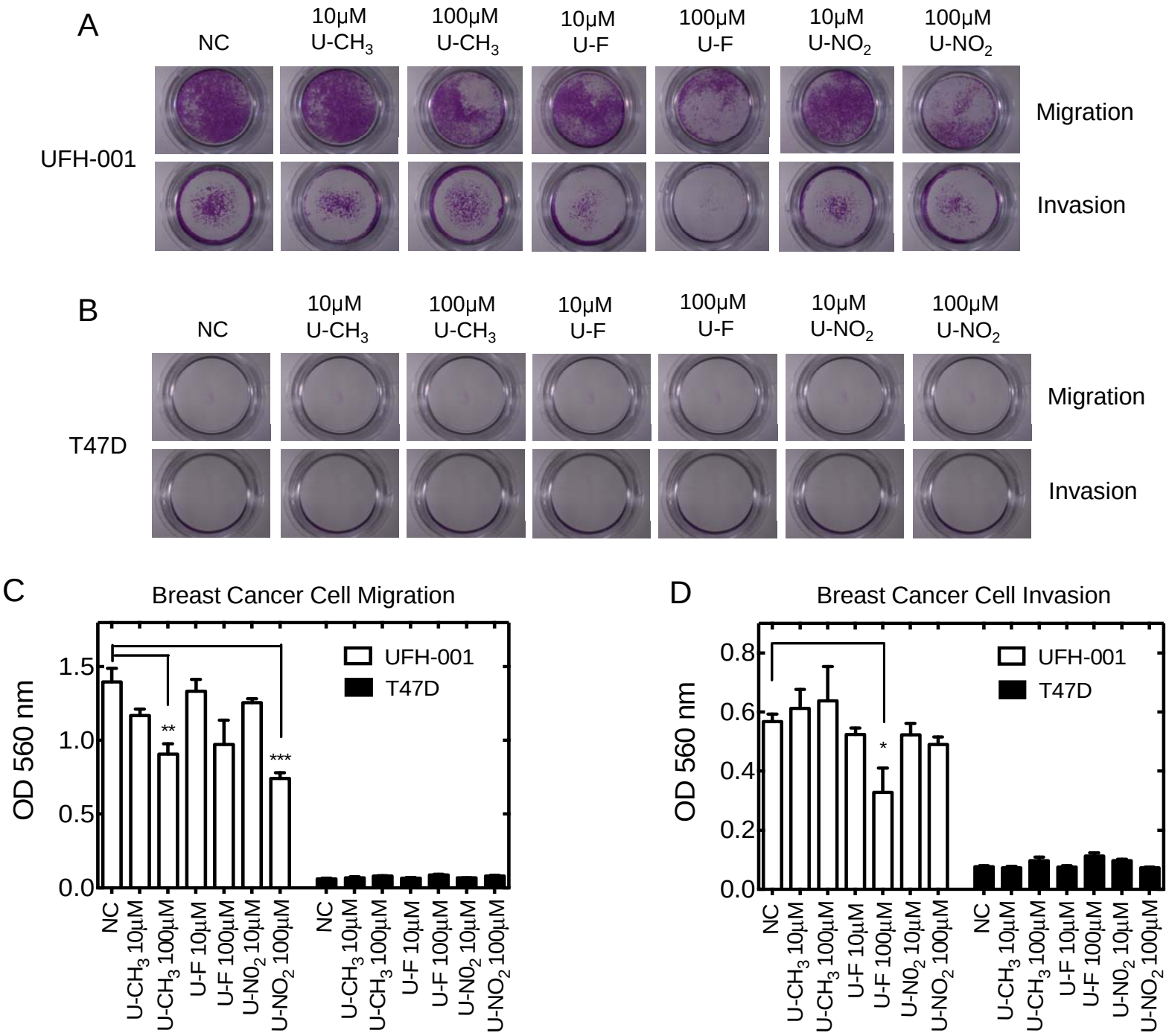
A
NC
10μM U-CH3
100μM U-CH3
10μM U-F
100μM U-F
10μM U-NO2
100μM U-NO2
UFH-001
Migration
Invasion
B
T47D
C
Breast Cancer Cell Migration
OD 560 nm
UFH-001
T47D
**
***
D
Breast Cancer Cell Invasion
*

Fig.8